Functionalizing a dentin bonding resin to become bioactive

Tauböck, Tobias T ; Zehnder, Matthias ; Schweizer, Thomas ; Stark, Wendelin J ; Attin, Thomas ; Mohn, Dirk

Abstract: OBJECTIVES To investigate chemo-mechanical effects of incorporating alkaline bioactive glass nanoparticles into a light-curable dental resin matrix. METHODS An unfilled Bis-GMA/TEGDMA material was infiltrated with up to 20 wt% of ultrafine SiO2-Na2O-CaO-P2O5-Bi2O3 particles. The unfilled and filled resins were investigated regarding their viscosity before setting and compared to commercially available materials. Set specimens were immersed for 21 days in phosphate buffered saline at 37°C. Water uptake, pH, Knoop hardness, and degree of conversion of freshly polymerized and stored samples were investigated. Resin surfaces were viewed and mapped in a scanning electron microscope for the formation of calcium phosphate (Ca/P) precipitates. In addition, Raman spectroscopy was performed. Numeric values were statistically compared ($p<0.01$). RESULTS Viscosity increased with particle loading, but remained below that of a flowable dental composite material. Water uptake into and pH induction from the polymerized samples also increased with particle loading ($p<0.01$). The addition of 20 wt% nanoparticles had no significant influence on microhardness, yet it slightly ($p<0.01$) increased the degree of conversion after 21 days. Ca/P precipitates formed on specimens filled with 20 wt% of the particles, while they were scarce on counterparts loaded with 10 wt%, and absent on unfilled resin surfaces. SIGNIFICANCE The results of the current study show that a Bis-GMA-based resin can be functionalized using alkaline nanoparticles. A material with bioactive properties and similar hardness as the unfilled resin was obtained by incorporating 20wt% of ultrafine SiO2-Na2O-CaO-P2O5-Bi2O3 particles into the resin matrix.

DOI: https://doi.org/10.1016/j.dental.2014.05.029

Functionalizing a dentin bonding resin to become bioactive

Tobias T. Tauböck[1], Matthias Zehnder[1], Thomas Schweizer[2], Wendelin J. Stark[3], Thomas Attin[1], Dirk Mohn[1,3]

[1]Department of Preventive Dentistry, Periodontology and Cariology, Center for Dental Medicine, University of Zurich, Zurich, Switzerland

[2]Institute of Polymers, Department of Materials Science, ETH Zurich, Zurich, Switzerland

[3]Institute for Chemical and Bioengineering, Department of Chemistry and Applied Biosciences, ETH Zurich, Zurich, Switzerland

Short title: Bioactive glass infiltrated bonding resin

Corresponding author:

Dr. Dirk Mohn

Institute for Chemical and Bioengineering, Department of Chemistry and Applied Biosciences
ETH Zurich
Wolfgang-Pauli-Strasse 10
8093 Zurich
Switzerland

Department of Preventive Dentistry, Periodontology and Cariology
Center for Dental Medicine
University of Zurich
Plattenstrasse 11
8032 Zurich
Switzerland

E-mail: dirk.mohn@chem.ethz.ch
Phone: +41 44 633 45 14
Fax: +41 44 633 15 71

ABSTRACT

Objectives. To investigate chemo-mechanical effects of incorporating alkaline bioactive glass nanoparticles into a light-curable dental resin matrix.

Methods. An unfilled Bis-GMA/TEGDMA material was infiltrated with up to 20 wt% of ultrafine SiO_2-Na_2O-CaO-P_2O_5-Bi_2O_3 particles. The unfilled and filled resins were investigated regarding their viscosity before setting and compared to commercially available materials. Set specimens were immersed for 21 days in phosphate buffered saline at 37°C. Water uptake, pH, Knoop hardness, and degree of conversion of freshly polymerized and stored samples were investigated. Resin surfaces were viewed and mapped in a scanning electron microscope for the formation of calcium phosphate (Ca/P) precipitates. In addition, Raman spectroscopy was performed. Numeric values were statistically compared ($p < 0.01$).

Results. Viscosity increased with particle loading, but remained below that of a flowable dental composite material. Water uptake into and pH induction from the polymerized samples also increased with particle loading ($p < 0.01$). The addition of 20 wt% nanoparticles had no significant influence on microhardness, yet it slightly ($p < 0.01$) increased the degree of conversion after 21 days. Ca/P precipitates formed on specimens filled with 20 wt% of the particles, while they were scarce on counterparts loaded with 10 wt%, and absent on unfilled resin surfaces.

Significance. The results of the current study show that a Bis-GMA-based resin can be functionalized using alkaline nanoparticles. A material with bioactive properties and similar hardness as the unfilled resin was obtained by incorporating 20 wt% of ultrafine SiO_2-Na_2O-CaO-P_2O_5-Bi_2O_3 particles into the resin matrix.

Keywords: bioactive filler, bioglass, nanoparticles, calcium phosphate, Bis-GMA/TEGDMA, composite material, microhardness.

1. Introduction

Among the various agents that have been used to cover exposed dentin, resin-based materials and glass-ionomer cements are the most widely used in restorative dentistry [1]. Originally, it was attempted to render these materials as inert as possible [2]. However, more recent advances have included the functionalization of traditional dental materials for their specific application [3,4]. For materials with a direct contact to dentin, bioactivity, i.e. the induction of calcium phosphate (Ca/P) precipitates, might be a desirable feature. Calcium and phosphorus species released from such bioactive materials could occlude dentinal tubules [5] and/or remineralize carious dentin [6]. A further distinct effect of alkaline biomaterials such as bioactive glasses of the 45S5 type is their induction of a high-pH environment, which renders these materials antimicrobial [7,8].

Alkaline bioactive glasses have been introduced first into glass-ionomer cements [9]. The water-permeability of these cements [10] would make them first choice for the incorporation of hydrophilic particles such as bioactive glass. However, the high alkalinity of bioactive glasses of the 45S5 type, i.e. SiO_2-Na_2O-CaO-P_2O_5 mixture, compromises the mechanical properties of the resulting glass-ionomer cements [11]. Apparently, the alkaline particles interfere with the acid-base reaction between the acidic polyelectrolyte and the aluminosilicate glass. On the other hand, nanometric bioactive glass 45S5 can be successfully embedded into a polyisoprene matrix to obtain a potential root-filling material with bioactive features [12,13]. It has been shown that the application of nanosized bioactive glass particles in biopolymers is in favor compared to micronsized particles in terms of wettability, pH induction and mechanical properties of the resulting composite [14]. Interestingly, it has never been investigated whether such ultrafine bioactive glass particles could be incorporated into dimethacrylate-based dental resins.

The hypothesis tested here was that resin polymerization is not impacted by alkaline nanometric bioactive glass particles, and that these particles embedded in the matrix would continue to exert bioactivity.

2. Materials and methods

2.1. Material preparation

Nanosized, radio-opaque bioactive glass particles were produced by flame spray synthesis [15]. In brief, corresponding metal precursors were combined and combusted in a flame spray setup to result in radio-opaque bioactive glass particles made up of a mixed oxide: SiO_2-Na_2O-CaO-P_2O_5-Bi_2O_3 [16]. The bioactive glass used in this study contained 20 wt% bismuth oxide to render the final composite visible on X-ray images. In the remaining 80 wt%, components were combined as in the classic 45S5 bioactive glass [17]: 45% SiO_2, 24.5% Na_2O, 24.5% CaO and 6% P_2O_5 (all in wt%). The particles were collected on a filter, mounted above the flame, sieved (300 μm) and used as received (30–50 nm particle size). The dentin bonding agent Heliobond (Ivoclar Vivadent, Schaan, Liechtenstein; lot: R02303), a mixture of 60 wt% bisphenol-A-glycidyldimethacrylate (Bis-GMA) and 40 wt% triethylene glycol dimethacrylate (TEGDMA), was used as polymeric matrix [18] and infiltrated with 0, 10 or 20 wt% bioactive glass using a dual asymmetric centrifuge (Speedmixer DAC 150, Hauschild Engineering, Hamm, Germany) at 3500 revolutions per minute for 60 s.

2.2. Viscosity assessment before curing

Combined Heliobond and bioactive glass with a loading of 0, 10 and 20 wt% (prepared as described above) were subjected to rheological analysis (Physica MCR 300, Anton-Paar, Zofingen, Switzerland) using a cone-plate geometry (30 mm diameter, 2° cone angle) at 25°C to determine the viscosity before curing. The space between cone and plate was filled completely with material and excess was removed. Shear rate ramp tests were performed with shear rates ranging from 0.1 to 100 s^{-1} (n = 3). The following commercial materials served as reference samples: a filled dentin bonding agent (Optibond FL, Kerr, Orange, CA, USA; lot: 4689425), a fissure sealant (Helioseal, Ivoclar Vivadent; lot: M69511) and a flowable

composite (Filtek Supreme XTE Flowable Restorative, 3M ESPE, St. Paul, MN, USA; lot: N368930).

2.3. Immersion in phosphate buffered saline

For this and all subsequent experiments, disk-shaped resin specimens (diameter: 6 mm, height: 2 mm) with three different loadings of bioactive glass (0, 10 and 20 wt%) were prepared in Teflon molds pressed between two glass plates, and light-cured for 5 min in a Spectramat SP1 curing unit (Ivoclar Vivadent) with a tungsten halogen light bulb (600 W, 220 V). Cured resin specimens were immersed in 1 mL phosphate buffered saline (PBS, GIBCO, Invitrogen, Billings, MT, USA) at pH 7.4 and 37°C for 21 days without changing the aqueous medium.

2.4. pH measurements

The pH (n = 3) was monitored using a calibrated pH electrode (Seven Easy, Mettler Toledo, Greifensee, Switzerland) after 0.5, 1, 2, 4, 8 h, 1, 3, 7, 14 and 21 days. Mere PBS served as a reference for pH measurements.

2.5. Water uptake

Additionally, the ability of the resin specimens to take up water was calculated by the wet weight W_{wet} (determined after the specimens were removed from the liquid, dipped thrice in distilled water and carefully blotted dry) and the dry weight W_{dry} (determined after vacuum drying during 7 days at room temperature of 23°C). The water uptake (WU) was calculated according to the following equation:

$$WU\ (\%) = \frac{W_{wet} - W_{dry}}{W_{dry}} \cdot 100$$

All measurements were performed in triplicates using a precision balance (XS 205, Mettler-Toledo).

2.6. Determination of microhardness

Knoop hardness was measured 24 h after photoactivation, and after 21 days of immersion in PBS at 37°C using a digital microhardness tester (model no. 1600-6106, Buehler, Lake Bluff, IL, USA). For each specimen (n = 3), three indentations were performed under a load of 100 g applied for 20 s at random positions around the center of the irradiated resin surface, and the average of the three readings was calculated.

2.7. Degree of conversion analysis

Degree of conversion (DC) of the filled and unfilled resins was assessed both before and after immersion in PBS using a Fourier transform infrared spectrometer (Vertex 70, Bruker, Fällanden, Switzerland) equipped with an attenuated total reflectance device with a single platinum crystal. Spectra were recorded from 400 to 4000 cm^{-1} with 64 scans and a resolution of 4 cm^{-1}. The DC was calculated from the ratio of absorbance intensities of aliphatic C=C stretching vibrations (peak height at 1637 cm^{-1}) and aromatic C–C stretching vibrations (peak height at 1608 cm^{-1}, internal standard) between the polymerized and unpolymerized samples [19]. Experiments were performed in triplicates.

2.8. Surface analysis

Specimens were mounted on aluminum stubs (12 mm) with the aid of carbon tape and sputtered with 5 nm platinum. A Nova NanoSEM 450 (FEI, Eindhoven, The Netherlands)

scanning electron microscope (SEM) was operated at 3 kV for observational scans to assess surface morphology before and after immersion in PBS. Energy-dispersive X-ray spectroscopy (EDX) was performed at 10 kV to investigate elemental composition of the specimens. Additionally, Raman spectroscopy was carried out with 785 nm excitation wavelength using a NIR laser at a power of 300 mW and 100% intensity (inVia Raman Microscope, Renishaw, New Mills, United Kingdom). Spectra were recorded on dry specimens from 500 to 1500 cm^{-1} with a spot size of 638 nm, with a spectral resolution of 1 cm^{-1} and without baseline correction.

2.9. Data presentation analysis

Values related to pH are presented using descriptive statistics. Viscosity, water uptake, Knoop hardness and degree of conversion values were evenly distributed (Shapiro-Wilk test), and thus compared with one-way ANOVA followed by Tukey's HSD post-hoc test. The α-type error was set at 0.01 for all statistical analyses ($p < 0.01$).

3. Results

Mere resins, such as Heliobond and Helioseal, showed stable viscosity under different shear rates. In comparison, loaded Heliobond as well as Filtek Supreme XTE Flowable Restorative showed a shear rate dependent viscosity (Table 1). 10 wt% loading of bioactive glass showed a minor increase in viscosity compared to pure Heliobond, while the 20 wt% loading raised the viscosity closer to the flowable composite (Filtek Supreme XTE Flowable Restorative) (Table 1).

Immersing the cured composite specimens in PBS revealed a sharp pH rise for both bioactive glass loadings, while pure Heliobond did not alter the pH (7.2) of the PBS solution. The specimens containing 10 wt% of the particles induced a pH increase to 8.7, which then decreased slightly (Fig. 1). In contrast, 20 wt% particle loading resulted in a pH of 10.8, which stayed constant during the 21-day period (Fig. 1).

Water sorption of the specimens increased with time in PBS and with higher particle loading. Mere Heliobond took up 3.2 ± 0.1 wt% water during the first 7 days, and 4.1 ± 0.3 wt% after 21 days. Composite loadings of 10 wt% bioactive glass resulted in 6.9 ± 0.4 wt% and 8.5 ± 0.4 wt% water uptake, respectively. Increasing the particle loading to 20 wt%, raised the water uptake to 9.5 ± 0.3 wt% and 12.8 ± 0.1 wt%, respectively. The differences between the different loadings at the respective times were statistically significant ($p < 0.01$).

Initial microhardness was statistically similar for polymerized Heliobond with or without particles ($p > 0.01$). The same held true for the DC. The mere polymer and the bioactive glass-filled specimens became significantly harder after 21 days of immersion in PBS (Fig. 2, left). This significant increase ($p < 0.01$) was also observed for the DC (Fig. 2, right). After 21 days of immersion, Knoop hardness was again similar between the experimental groups ranging between 20.4 ± 0.3 and 22.7 ± 0.6 KHN. However, a small, yet significant ($p < 0.01$) difference was observed between the unfilled polymer and the

counterpart loaded with 10 wt% of the particles. In contrast, the DC of the 20 wt% bioactive glass-loaded composite was significantly higher ($p < 0.01$) compared to that of both the 10 wt% loaded composite and the unfilled resin.

As observed by SEM, mere polymer represented a relative smooth surface (Fig. 3a), while incorporated spherical bioactive glass particles were evenly distributed at the surface (Fig. 3c). Calcium phosphate crystals were observed after 21 days of immersion in PBS with 20 wt% bioactive glass (Fig. 3d). In contrast, pure Bis-GMA/TEGDMA specimens (no particles) showed a somewhat eroded surface, without precipitates (Fig. 3b). The specimens containing 10 wt% of the bioactive particles showed scattered precipitates (not shown), but lacked the even appearance of counterparts loaded with 20 wt%. Elemental point analysis (Fig. 4) revealed a high calcium phosphate concentration on the surface of 20 wt% bioactive glass-loaded specimens after immersion in PBS for 21 days compared to as-prepared specimens. Neither calcium nor phosphorous was detected for mere polymer specimens. This was also corroborated by Raman spectroscopy. A phosphate peak appeared after 21 days of immersion in PBS (Fig. 5), while a small carbonate peak disappeared for particle-loaded specimens. Other major peaks belong to the resin matrix composed of Bis-GMA/TEGDMA: 610 cm^{-1} (C-C=O bend, methacrylate), 830 cm^{-1} (C-O-C bend), 1130 cm^{-1} (phenyl, C-O-C), 1190 cm^{-1} (CH_3-C-CH_3), 1470 cm^{-1} (CH_2, CH_3 asymmetric bend) [20, 21].

4. Discussion

The current study showed, for the first time, that nanoparticulate bioactive glass particles can be incorporated into a Bis-GMA/TEGDMA matrix and still induce reactivity in an aqueous environment. This result was not readily foreseeable, as the particles are highly hydrophilic and alkaline. Increasing the amount of these particles renders the functionalized polymer more bioactive [22], yet appears to have little effect on hardness and monomer conversion of the photopolymerized material. Viscosity of the unset material, however, is also affected by the bioactive glass particles in a dose-dependent manner.

The work presented in the current paper was a pure laboratory study. Since it was not clear how alkaline hydrophilic particles such as the tailored 45S5 bioglass powder used here would affect a hydrophobic matrix, it was necessary to investigate the basic properties of the resulting composite material. Unset Bis-GMA/TEGDMA specimens loaded with 10 or 20 wt% bioactive glass showed higher viscosities (Table 1) at shear rates between 0.1 and 100 s^{-1} than a commercial barium-glass-filled bonding agent (Optibond FL), despite the higher filler content (48%) of the latter material. A recent study found no correlation between filler load and rheological behavior of dimethacrylate-based resins [23], suggesting that the viscosity of these materials might be more linked to the filler type and size than to the amount of filler included. Additionally, the nanoparticulate size of the applied particles and a further optimized particle tailoring (e.g. silanization) could improve the homogeneity of particle dispersion and viscosity. Nevertheless, even with 20 wt% particle loading, the experimental composite material only reached about half the viscosity of a commercial flowable resin composite (Filtek Supreme XTE Flowable Restorative), when evaluated at a frequency of 10 rad/s, which is approximating the clinical application [24]. Whether this viscosity would allow for adequate penetration of the functionalized polymer into dentin substrates needs to be investigated in a future study.

Microhardness of both unfilled and filled Bis-GMA/TEGDMA specimens increased with time during the three-week storage period (Fig. 2, left). This observation might be explained by the phenomenon of post-cure, resulting in a continuous cross-linking process of the resin phase after photoactivation and an increase of monomer conversion over time [25]. In accordance with the current results, previous studies found substantial increases in composite hardening, even 24 h after irradiation [26,27]. Usually, hardness as well as other mechanical properties of resin-based materials improve with increasing filler loading [28,29]. This was also observed in a recent study on the incorporation of bioactive glass fillers into a resin matrix [22]. In the present study, however, resin specimens infiltrated with nanoparticulate bioactive glass particles attained similar hardness values as the unfilled polymer both before and after 21 days of immersion in PBS, probably because non-silanized glass particles were used, which might have prevented optimal filler-to-matrix integrity. It would appear that the most influential factor on the microhardness of these specimens was the matrix rather than the filler content.

As expected, pH induction was affected by the bioactive glass particles in a dose-dependent manner. Apparently, the particles were evenly distributed in the matrix with a large active exchange surface of glass and surrounding liquid (Fig. 3c), which might have favored the establishment of a constant high-pH environment at 20 wt% loading during the three-week storage period in PBS (Fig. 1). Water sorption of the composite specimens also increased with higher particle loading due to the hydrophilicity of the nanoparticulate bioactive glass. The ability of bioactive glasses to raise the pH in aqueous suspensions, as a result of the release of alkali ions, mainly Na^+, and the incorporation of protons (H^+) into the corroding material, renders these particles antimicrobial [30,31]. The antimicrobial potential of nanometric 45S5 bioglass [32] makes the current composite an interesting candidate to be further tested as a dentin disinfectant, e.g. as a liner for step-wise caries excavation.

Ca/P crystals formed on the material loaded with 20 wt% particles appeared to be similar to crystals deposited on a pre-market material in a most recent study [13] under similar conditions. As specimens were immersed in PBS, which contains sodium, phosphate and chloride, but no calcium, precipitated calcium (as part of Ca/P crystals) had to be first released by bioactive glass and then re-precipitate from the aqueous solution [33]. This Ca/P layer formed a diffusion barrier and possibly retarded the dissolution of further ions from glass particles. The relatively low amount of calcium in the system (material and liquid) compared to the frequently used simulated body fluid (SBF) could result in Ca/Ps with lower calcium to phosphate molar ratios than the classical hydroxyapatite. In the here presented specimens, less apatite was formed compared to a study with similar composite systems [22], due to a different aqueous medium (PBS instead of SBF) and a shorter immersion time. The here observed precipitations showed similar crystal appearance as shown in most recent studies using PBS as an immersion liquid [33]. Taking SEM (Fig. 3) and EDX (Fig. 4) results together, the obtained data clearly showed precipitated Ca/P crystals [34]. Comparing EDX spectra of filled resin before and after immersion, considerable changes for Si, Ca and P were observed (Fig. 4, bottom). It was noticed that after immersion, the concentration of Si was reduced compared to the initial specimens, whereas the concentration of Ca and P increased with immersion in PBS. This observation and the appearing phosphate peak in the Raman spectra (Fig. 5) support the concept that a Ca/P layer was newly formed. In a most recent study [22], micronsized bioactive glass particles were incorporated in experimental resins (33 wt% particle loading). Although there were several differences between the two studies (filler loading, immersion time, immersion medium, replenishment of the liquid), the here presented data showed that the customized resins, including bioactive glass nanoparticles, possess bioactive properties next to the successful polymerization of the resins.

As suggested above, the material under investigation could be especially interesting to infiltrate dentin caries and/or as a dentin bonding agent. Another promising application could be the treatment of dentin hypersensitivity, a clinically unresolved problem. Resins applied to the exposed dentin may be washed out by the dentinal fluid or lost over time by oral hygiene measures [35]. Bioactive particles incorporated into a flowable resin could solve this problem by promoting dentinal tubule occlusion via the formation of Ca/P precipitates. Moreover, the interface between resin and dentin could become more durable [36]. Future studies should test these hypotheses.

5. Conclusion

Nanometric bioactive glass particles can be incorporated into a dimethacrylate-based dental resin. At 20 wt% loading, the nanoparticles appear to form a functional unit with the matrix, while 10 wt% loading may be too low to induce the desired effects in the set polymer. The functionalized Bis-GMA-based resin has bioactive properties, which should be explored *in situ*.

Acknowledgements

This study was supported by the authors' institutions. MZ, WJS and DM declare a financial interest in the form of a patent application (WO2011/020204) on radio-opaque bioactive glass licensed to smartodont llc., of which MZ, WJS and DM are shareholders.

References

[1] McLean JW. Dentinal bonding agents versus glass-ionomer cements. Quintessence Int 1996;27:659-67.

[2] Schmalz G. The biocompatibility of non-amalgam dental filling materials. Eur J Oral Sci 1998;106:696-706.

[3] Chen MH. Update on dental nanocomposites. J Dent Res 2010;89:549-60.

[4] Ferracane JL. Resin composite–State of the art. Dent Mater 2011;27:29-38.

[5] Mitchell JC, Musanje L, Ferracane JL. Biomimetic dentin desensitizer based on nano-structured bioactive glass. Dent Mater 2011;27:386-93.

[6] Vollenweider M, Brunner TJ, Knecht S, Grass RN, Zehnder M, Imfeld T, et al. Remineralization of human dentin using ultrafine bioactive glass particles. Acta Biomater 2007;3:936-43.

[7] Stoor P, Söderling E, Salonen JI. Antibacterial effects of a bioactive glass paste on oral microorganisms. Acta Odontol Scand 1998;56:161-5.

[8] Gubler M, Brunner TJ, Zehnder M, Waltimo T, Sener B, Stark WJ. Do bioactive glasses convey a disinfecting mechanism beyond a mere increase in pH? Int Endod J 2008;41:670-8.

[9] Yli-Urpo H, Närhi M, Närhi T. Compound changes and tooth mineralization effects of glass ionomer cements containing bioactive glass (S53P4), an in vivo study. Biomaterials 2005;26:5934-41.

[10] Jevnikar P, Jarh O, Sepe A, Pintar MM, Funduk N. Micro magnetic resonance imaging of water uptake by glass ionomer cements. Dent Mater 1997;13:20-3.

[11] Yli-Urpo H, Lassila LV, Närhi T, Vallittu PK. Compressive strength and surface characterization of glass ionomer cements modified by particles of bioactive glass. Dent Mater 2005;21:201-9.

[12] Mohn D, Bruhin C, Luechinger NA, Stark WJ, Imfeld T, Zehnder M. Composites made of flame-sprayed bioactive glass 45S5 and polymers: bioactivity and immediate sealing properties. Int Endod J 2010;43:1037-46.

[13] Marending M, Bubenhofer SB, Sener B, De-Deus G. Primary assessment of a self-adhesive gutta-percha material. Int Endod J 2013;46:317-22.

[14] Misra SK, Mohn D, Brunner TJ, Stark WJ, Philip SE, Roy I, et al. Comparison of nanoscale and microscale bioactive glass on the properties of P(3HB)/Bioglass composites. Biomaterials 2008;29:1750-61.

[15] Brunner TJ, Grass RN, Stark WJ. Glass and bioglass nanopowders by flame synthesis. Chem Commun 2006;13:1384-6.

[16] Mohn D, Zehnder M, Imfeld T, Stark WJ. Radio-opaque nanosized bioactive glass for potential root canal application: evaluation of radiopacity, bioactivity and alkaline capacity. Int Endod J 2010;43:210-7.

[17] Hench LL, Splinter RJ, Allen C, Greenlee TK. Bonding mechanisms at the interface of ceramic prosthetic materials. J Biomed Mater Res 1971;5:117-41.

[18] Schneider OD, Stepuk A, Mohn D, Luechinger NA, Feldman K, Stark WJ. Light-curable polymer/calcium phosphate nanocomposite glue for bone defect treatment. Acta Biomater 2010;6:2704-10.

[19] Moraes RR, Faria-e-Silva AL, Ogliari FA, Correr-Sobrinho L, Demarco FF, Piva E. Impact of immediate and delayed light activation on self-polymerization of dual-cured dental resin luting agents. Acta Biomater 2009;5:2095-100.

[20] Willis HA, Zichy VJI, Hendra PJ. The laser-Raman and infra-red spectra of poly(methyl methacrylate). Polymer 1969;10:737-46.

[21] Santini A, Miletic V. Quantitative micro-Raman assessment of dentine demineralization, adhesive penetration, and degree of conversion of three dentine bonding systems. Eur J Oral Sci 2008;116:177-83.

[22] Sauro S, Osorio R, Fulgencio R, Watson TF, Cama G, Thompson I, et al. Remineralisation properties of innovative light-curable resin-based dental materials containing bioactive micro-fillers. J Mater Chem B 2013;1:2624-38.

[23] Beun S, Bailly C, Devaux J, Leloup G. Physical, mechanical and rheological characterization of resin-based pit and fissure sealants compared to flowable resin composites. Dent Mater 2012;28:349-59.

[24] Lee IB, Son HH, Um CM. Rheologic properties of flowable, conventional hybrid, and condensable composite resins. Dent Mater 2003;19:298-307.

[25] Lopez-Suevos F, Dickens SH. Degree of cure and fracture properties of experimental acid-resin modified composites under wet and dry conditions. Dent Mater 2008;24:778-85.

[26] Watts DC, Amer OM, Combe EC. Surface hardness development in light-cured composites. Dent Mater 1987;3:265-9.

[27] Cassoni A, Ferla Jde O, Albino LG, Youssef MN, Shibli JA, Rodrigues JA. Argon ion laser and halogen lamp activation of a dark and light resin composite: microhardness after long-term storage. Lasers Med Sci 2010;25:829-34.

[28] Xu HH. Dental composite resins containing silica-fused ceramic single-crystalline whiskers with various filler levels. J Dent Res 1999;78:1304-11.

[29] Tauböck TT, Oberlin H, Buchalla W, Roos M, Attin T. Comparing the effectiveness of self-curing and light curing in polymerization of dual-cured core buildup materials. J Am Dent Assoc 2011;142:950-6.

[30] Allan I, Newman H, Wilson M. Antibacterial activity of particulate bioglass against supra- and subgingival bacteria. Biomaterials 2001;22:1683-7.

[31] Sepulveda P, Jones JR, Hench LL. In vitro dissolution of melt-derived 45S5 and sol-gel derived 58S bioactive glasses. J Biomed Mater Res 2002;61:301-11.

[32] Waltimo T, Brunner TJ, Vollenweider M, Stark WJ, Zehnder M. Antimicrobial effect of nanometric bioactive glass 45S5. J Dent Res 2007;86:754-7.

[33] Varila L, Fagerlund S, Lehtonen T, Tuominen J, Hupa L. Surface reactions of bioactive glasses in buffered solutions. J Eur Ceram Soc 2012;32:2757-63.

[34] Hong Z, Reis RL, Mano JF. Preparation and in vitro characterization of novel bioactive glass ceramic nanoparticles. J Biomed Mater Res A 2009;88:304-13.

[35] Ferrari M, Cagidiaco MC, Kugel G, Davidson CL. Clinical evaluation of a one-bottle bonding system for desensitizing exposed roots. Am J Dent 1999;12:243-9.

[36] Profeta AC, Mannocci F, Foxton R, Watson TF, Feitosa VP, De Carlo B, et al. Experimental etch-and-rinse adhesives doped with bioactive calcium silicate-based micro-fillers to generate therapeutic resin-dentin interfaces. Dent Mater 2013;29:729-41.

Figure captions

Fig. 1 – pH evolution (mean ± standard deviation) of phosphate-buffered saline (PBS) containing unfilled and filled Bis-GMA/TEGDMA specimens up to 21 days at 37°C (n = 3). BG: bioactive glass.

Fig. 2 – Development of post-irradiation surface Knoop microhardness (left, mean ± standard deviation) and degree of conversion (right, mean ± standard deviation) of unfilled and filled Bis-GMA/TEGDMA specimens during the 21-day storage period (n = 3). BG: bioactive glass.

Fig. 3 – Overview of scanning electron microscopy images of mere Bis-GMA/TEGDMA 24 h after photoactivation (a), and after immersion in phosphate buffered saline (PBS) for 21 days showing a somewhat eroded surface (b). 20 wt% loading of bioactive glass in Bis-GMA/TEGDMA 24 h after photoactivation (c) and after immersion in PBS for 21 days showing calcium phosphate precipitates (d); elemental mapping of the corresponding element; insert: higher magnification. BG: bioactive glass.

Fig. 4 – Elemental analysis of unfilled and filled Bis-GMA/TEGDMA specimens showing the different elemental distributions on the surfaces of the experimental samples. BG: bioactive glass; PBS: phosphate buffered saline.

Fig. 5 – Raman spectroscopy of as-prepared specimens and after immersion in PBS for 21 days, showing the appearance of phosphate (960 cm^{-1}) and disappearance of carbonate (1080 cm^{-1}) for particle-loaded specimens. BG: bioactive glass; PBS: phosphate buffered saline.

Table 1 – Mean (± standard deviation) viscosities (in Pa s) of the experimental and commercial materials (n = 3) at different shear rates.

	Shear Rate [s^{-1}]			
Material	**0.1**	**1.0**	**10**	**100**
Optibond FL	1.47 (0.25)^{C,a}	1.40 (0.01)^{B,a}	1.27 (0.01)^{C,a}	1.20 (0.00)^{CD,a}
Helioseal	0.66 (0.19)^{C,a}	0.61 (0.02)^{B,a}	0.59 (0.00)^{C,a}	0.58 (0.01)^{D,a}
Heliobond	0.84 (0.54)^{C,a}	0.48 (0.11)^{B,a}	0.53 (0.02)^{C,a}	0.55 (0.00)^{D,a}
10 wt% BG in Heliobond	3.84 (0.69)^{C,b}	5.58 (0.10)^{B,a}	2.63 (0.06)^{C,bc}	1.55 (0.03)^{C,c}
20 wt% BG in Heliobond	249.01 (41.21)^{B,a}	123.90 (23.69)^{A,b}	19.93 (2.81)^{B,c}	5.40 (0.47)^{B,c}
Filtek Supreme XTE Flowable Restorative	445.87 (0.70)^{A,a}	99.00 (5.21)^{A,b}	36.34 (0.90)^{A,c}	16.83 (0.19)^{A,d}

BG: bioactive glass.
Mean values followed by same superscript capital letters in columns, and same superscript small letters in rows, are not significantly different at the 0.01 level (Tukey's HSD post-hoc test).

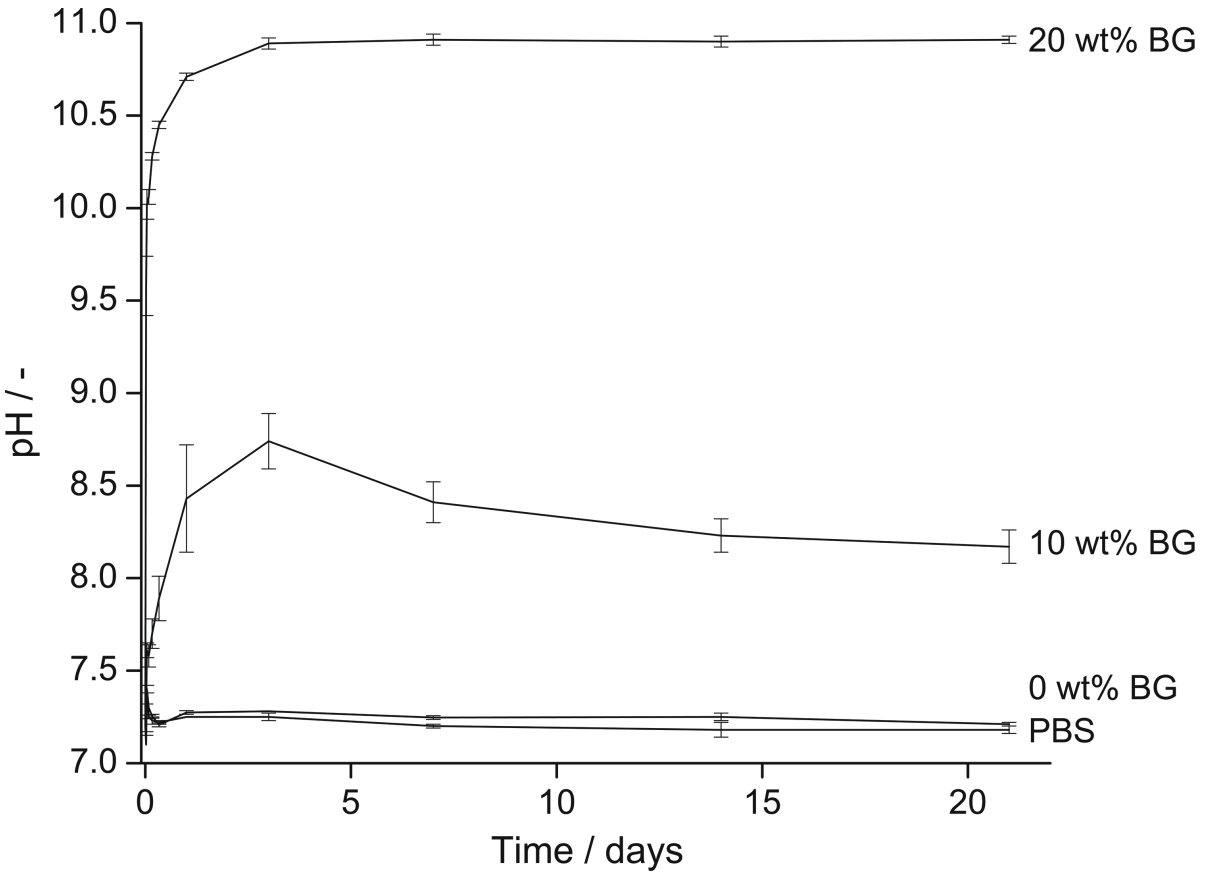

Fig. 1 – pH evolution (mean ± standard deviation) of phosphate-buffered saline (PBS) containing unfilled and filled Bis-GMA/TEGDMA specimens up to 21 days at 37°C (n = 3). BG: bioactive glass.

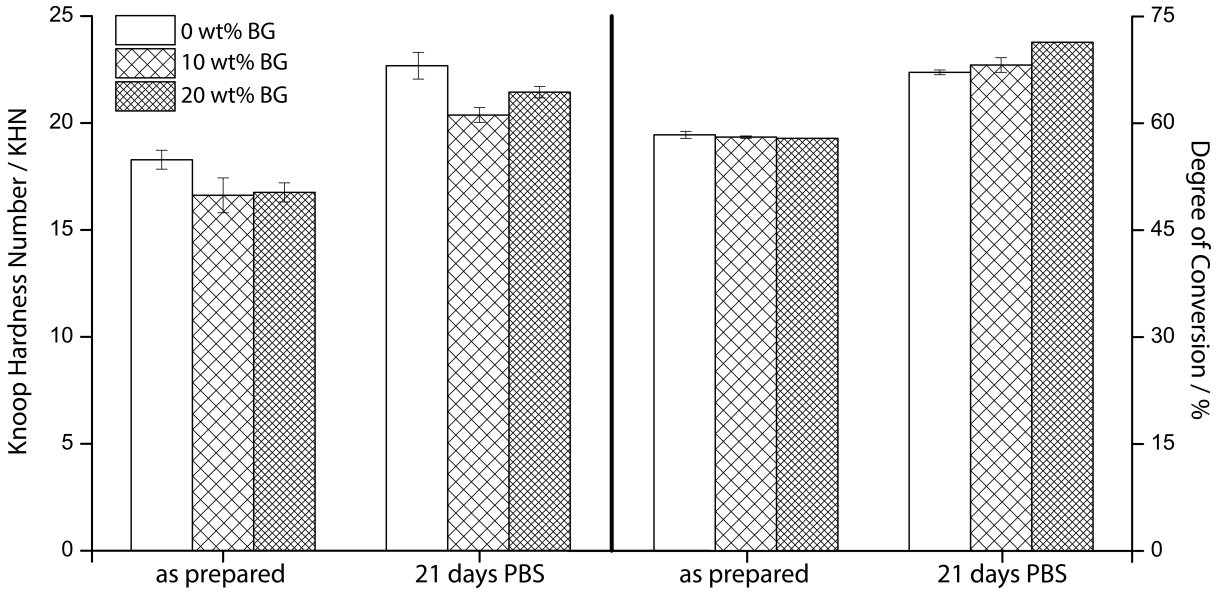

Fig. 2 – Development of post-irradiation surface Knoop microhardness (left, mean ± standard deviation) and degree of conversion (right, mean ± standard deviation) of unfilled and filled Bis-GMA/TEGDMA specimens during the 21-day storage period (n = 3). BG: bioactive glass.

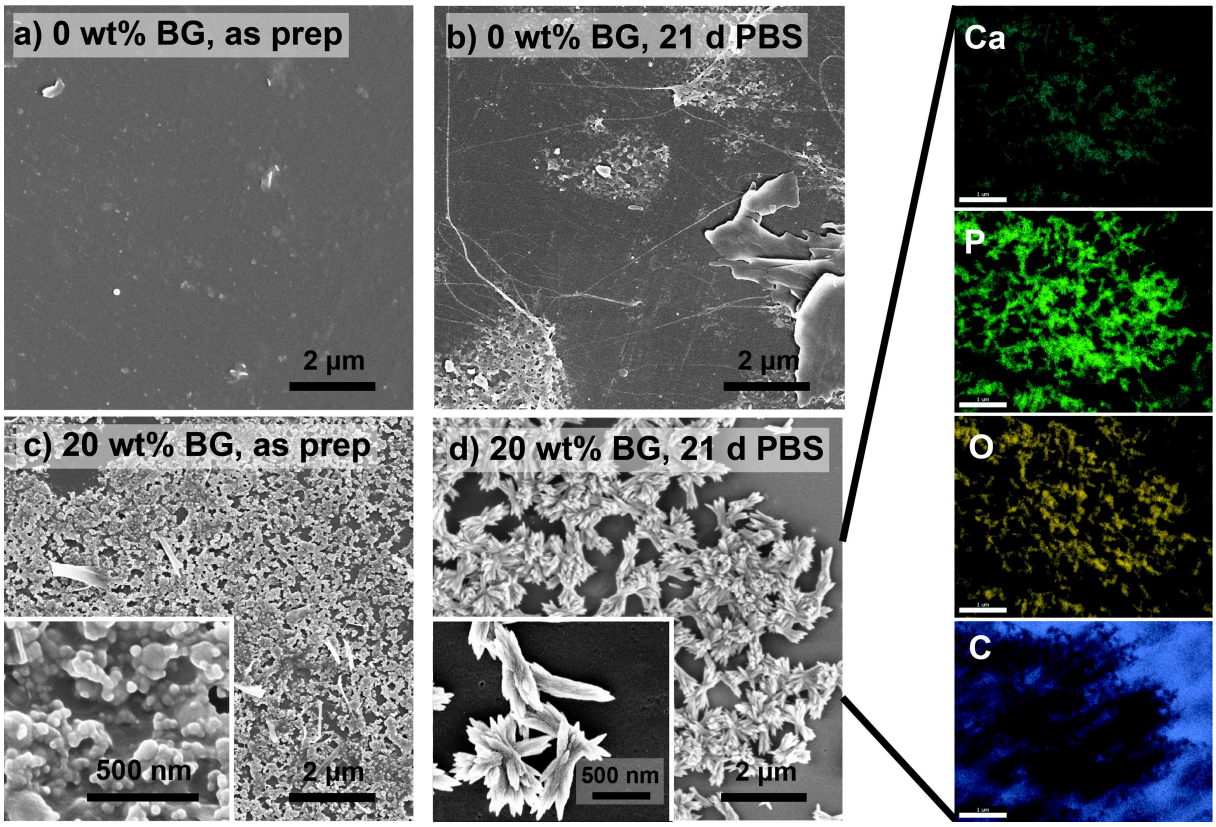

Fig. 3 – Overview of scanning electron microscopy images of mere Bis-GMA/TEGDMA 24 h after photoactivation (a), and after immersion in phosphate buffered saline (PBS) for 21 days showing a somewhat eroded surface (b). 20 wt% loading of bioactive glass in Bis-GMA/TEGDMA 24 h after photoactivation (c) and after immersion in PBS for 21 days showing calcium phosphate precipitates (d); elemental mapping of the corresponding element; insert: higher magnification. BG: bioactive glass.

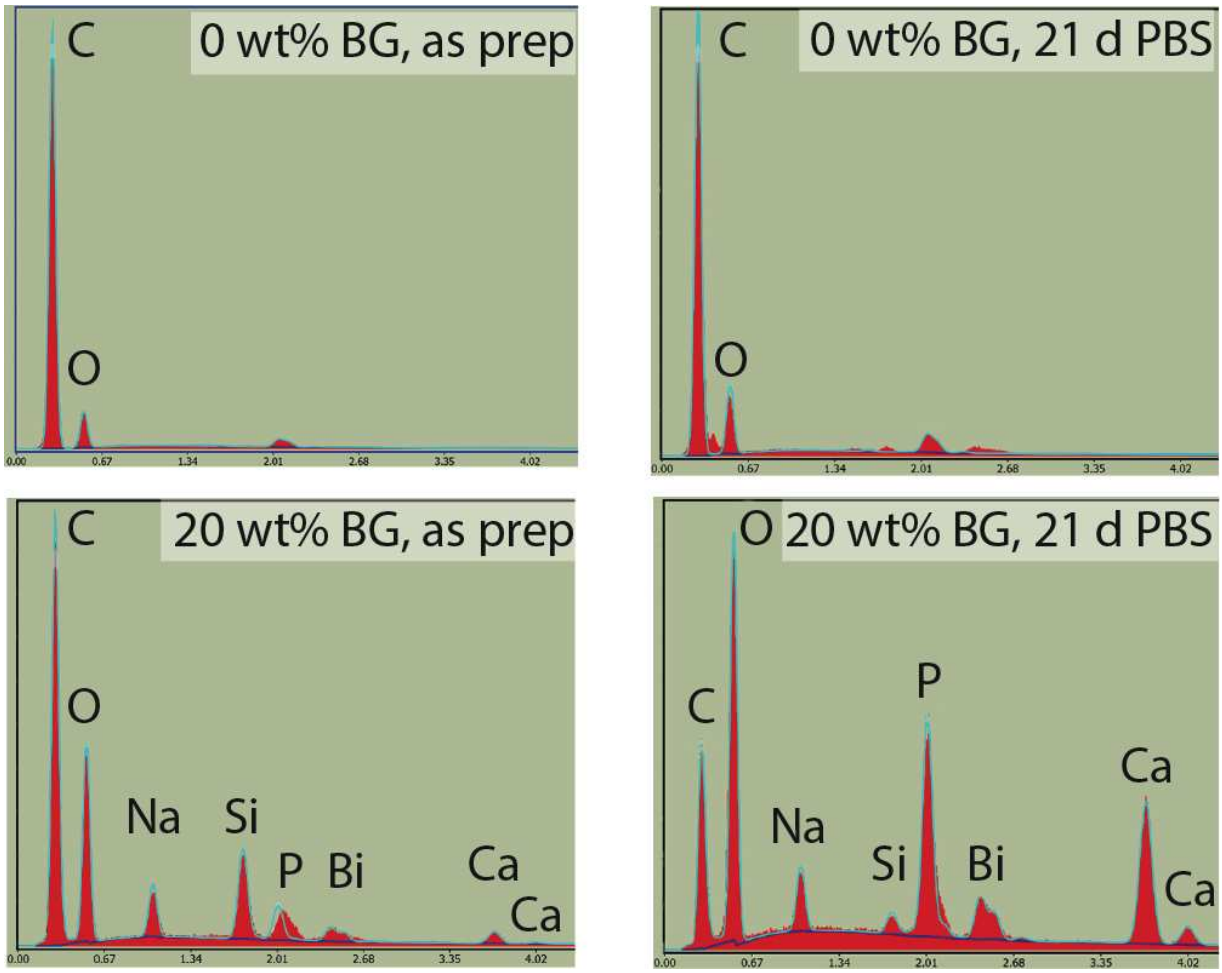

Fig. 4 – Elemental analysis of unfilled and filled Bis-GMA/TEGDMA specimens showing the different elemental distributions on the surfaces of the experimental samples. BG: bioactive glass; PBS: phosphate buffered saline.

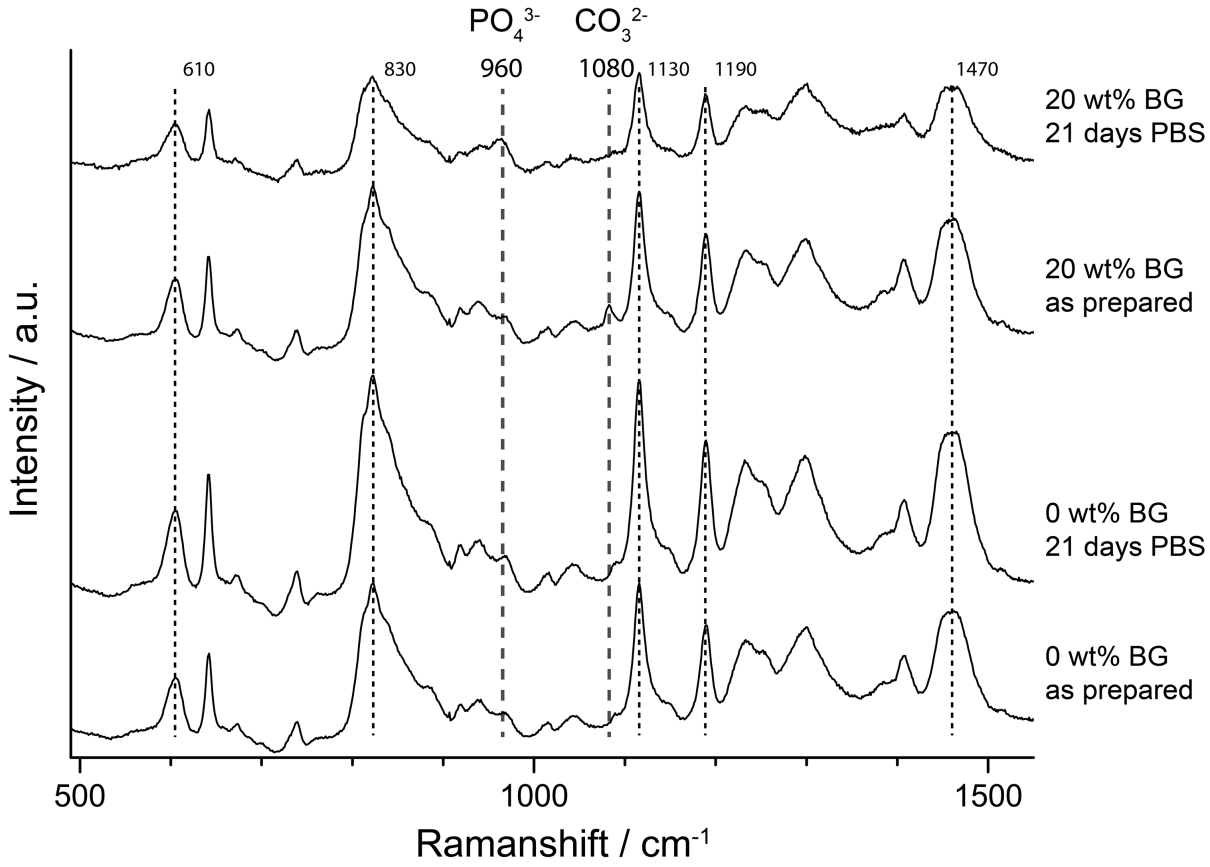

Fig. 5 – Raman spectroscopy of as-prepared specimens and after immersion in PBS for 21 days, showing the appearance of phosphate (960 cm^{-1}) and disappearance of carbonate (1080 cm^{-1}) for particle-loaded specimens. BG: bioactive glass; PBS: phosphate buffered saline.